Pyrometry for Turbine Blade Development

E. Suarez* and H. R. Przirembel†
Pratt and Whitney, West Palm Beach, Florida

This paper discusses the use of pyrometry for turbine health monitoring and experimental substantiation of turbine heat transfer models and designs. It also addresses techniques to correct for high levels of combustor reflection and random flame spikes. An overview of the technical issues involved in the use of pyrometry on ceramic coatings is also presented.

Nomenclature

E_f = total blade radiance in filtered band
E_{fb} = blade-emitted radiation in filtered band
E_{fr} = blade-reflected radiation in filtered band
E_s = reflection-corrected radiative signal
E_u = total blade radiance in unfiltered band
E_{ub} = blade-emitted radiation in unfiltered band
E_{ur} = blade-reflected radiation in unfiltered band

Introduction

AIRFOIL temperature distributions under actual engine pressure levels, gas stream turbulence, combustor radial profile, and external boundary-layer heat transfer coefficient are a critical aspect of any turbine development program. The optical pyrometer has proven to be a valuable tool for obtaining experimental substantiation without the expense of prolonged engine durability testing. The conventional measurement technique using embedded thermocouples requires grooving the thin airfoil sidewall, creating undesirable stress concentrations. Furthermore, durability at high temperature is limited, and signal transmission using a slipring or telemetry is expensive and complex. Other techniques such as thermal paints have been used successfully but do not offer the versatility of pyrometers.

Pyrometers in jet engines are subject to reflection from the combustor and emission from burning particles in the field of view. Engine data indicate good agreement between thermocouples and reflection-corrected data using the Dual Spectral Area technique. The error due to burning particles in the field of view is corrected under engine steady-state conditions by discarding the affected data and replacing it in subsequent revolutions.

Thermal barrier coatings (composites of ceramic and metallic underlayers) are translucent and have low emittance in the wavelength region currently being used and become opaque in the 8–12 μ range. These characteristics require a new measurement approach to obtain the surface temperature of coated turbine blades.

Pyrometer System

Principle of Operation

Radiation pyrometry provides a means for surface temperature measurement without perturbing the surface or surrounding medium. The pyrometer operates by collecting thermal radiation from a confined surface area that is optically transferred to a detector to produce an electrical signal proportional to the radiant power. The signal is related to a surface temperature by using Planck's law of radiation and appropriate corrections for surface emissivity. Measurement accuracy depends on the radiative properties of the surface, the medium in the optical path, instrument frequency response, and calibration.

Conventional ratio and single-band pyrometers have limited application in the turbine section of hydrocarbon-fueled jet engines. The presence of reflected radiation from the engine combustor significantly contributes to the radiation emitted by the surface, resulting in an erroneously high temperature indication. Spectral radiation measurements in current test and production engines indicate that as much as 70% of the radiant flux collected by the pyrometer between the wavelengths 0.35 and 1.15 μ can be reflected energy. At this level of reflected energy, a pyrometer viewing a surface with an actual temperature of 1800°F would indicate a temperature 200°F higher. Measurement devices such as the dual spectral area pyrometer (DSAP) have the capability of correcting for this reflected radiation.

The reflection correction technique of the DSAP[1,2] is based on the principle that two blackbody calibrated pyrometers, sensitive to different spectral wavelengths, will not respond equally when subjected to a radiative signal containing surface-emitted and reflected radiation from a significantly higher temperature source. The spectral ranges of operation of the pyrometers were selected to provide sufficient sensitivity between the surface-emitted radiation and the reflected component. The spectral ranges for the silicon detectors being used are 0.35–0.85 and 0.35–1.15 μ. In this paper, the 0.35–0.85 μ band will be called the filtered band, whereas the 0.35–1.15 μ band will be called the unfiltered band.

The magnitude of the displayed temperature difference between the two pyrometers is an indication of the magnitude of the reflected component. The amount of temperature correction is determined using this temperature difference, subject to the following assumptions and conditions:

1) The spectral characteristics of the source of reflection are constant and significantly different from that of the blade.

2) All surfaces are gray and have relatively high emissivities.

3) There are no large temperature differences between the surface being measured and the immediate surrounding surfaces.

Combustor Reflection

The accuracy of the DSAP correction technique is dependent on knowledge of the source of reflection. High levels of reflection coupled with the uncertainty of the spectral characteristics of the reflected component lead to significant errors. Figure 1 depicts the correction error as a function of the level of reflection present in the unfiltered band and combustor radiance temperature. The plot was generated for a 1900°F

Presented as Paper 88-3036 at the AIAA/ASME/SAE/ASEE 24th Joint Propulsion Conference, Boston, MA, July 11-13, 1988; received Sept. 16, 1988; revision received July 26, 1989.

*Project Engineer. Instrumentation Development.
†Project Engineer. Turbine Group, Component Design Technology.

blade surface temperature for which all reflected radiation was corrected assuming the combustor radiance temperature to be constant at 3800°F. The correction error corresponds to the difference between the actual blade temperature, 1900°F, and that calculated by the DSAP technique. The error increases with the level of reflection and the deviation from the assumed combustor radiance temperature.

The spectral characteristics of the combustor emittance are measured looking directly at the combustor fireball with a pyrometer installation similar to that used for the turbine blades. For this application, the pyrometer is calibrated with the input radiative power attenuated to provide a range of operation from 3200-4400°F. The combustor radiation in both spectral bands is recorded, and the ratio between bands computed for each data point is sampled every 5 μs. The equivalent blackbody temperature for each ratio is determined from the pyrometer calibration. The resulting combustor radiance temperature is used to correct for reflection by assuming that all surfaces involved in the radiative interchange are gray; that is, there are no significant spectral differences between the radiation emitted by the combustor and that reflected by the blade. Only the intensity of the radiation varies. Figure 2 shows a typical plot of combustor emission for both spectral bands as a function of time. Data recorded in F-100 engines indicate the average radiance temperature to be about 3820°F, varying between a maximum of 4020°F to a minimum of 3620°F. This fluctuation results in a correction error of ±50°F at 70% reflection and ±20°F at 50%. To achieve a correction accuracy of ±25°F at 70% reflection, the fireball temperature must be known within ±60°F. Frequency analysis indicates that the signal is generally wideband in nature.

Dual Spectral Area Algorithm

The dual spectral area correction technique uses a simple algorithm that subtracts from the total radiative signal the reflected component from a source at a significantly higher temperature than the surface being measured. The correction is performed to radiant power signals where the relationships among the various terms and contributions are linear.

The total output signal for the unfiltered band E_u (0.35-1.15 μ) is the sum of the blade emission E_{ub}, and the reflected component E_{ur}, namely

$$E_u = E_{ub} + E_{ur} \tag{1}$$

Similarly, the total output signal for the filtered band (0.35-0.85 μ) is expressed by

$$E_f = E_{fb} + E_{fr} \tag{2}$$

and E_s is defined by the expression

$$E_s = E_u - (E_{ur}/E_{fr})E_f \tag{3}$$

The quantity in parenthesis is the ratio of the combustor reflection in the measurement bands. The value is assumed to remain constant and is obtained by direct viewing of the combustor. The right-hand side of Eq. (3) is expanded to yield:

$$E_u - (E_{ur}/E_{fr})E_f = E_{ub} - (E_{ur}/E_{fr})E_{fb} \tag{4}$$

The left-hand side of Eq. (4) involves the pyrometer input radiation, containing both reflection and blade-emitted radiation, whereas the right-hand side only relates to blade emission. By the use of Eq. (4), the input signal has been expressed in terms of blade emission, and, consequently, reflection-corrected blade temperature. Figure 3 depicts the relation between the corrected blade temperature and the quantity E_s. Although the relation is double valued, in practice E_u and E_f are limited by the dynamic range of the electronic components. This in turn limits the range of E_s, resulting in a one-to-one relationship with blade temperature as shown in Fig. 4.

Since E_s is an indication of corrected blade temperature, it is used for engine control without further processing.

Signal Saturation and Processing

Signal saturation occurs when large quantities of radiation are present in the pyrometer field of view, overpowering all blade emission. This also occurs when the reflected compo-

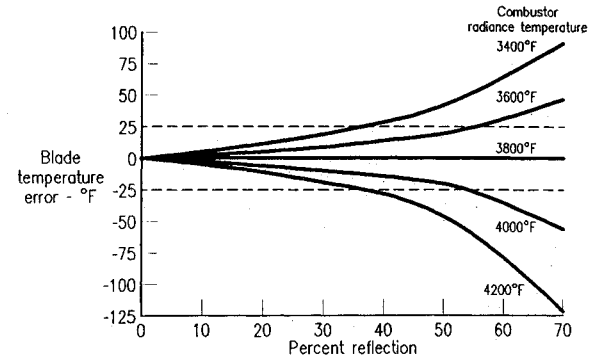

Fig. 1 Effect of variable combustor radiance temperature and reflection level on the accuracy of blade temperature.

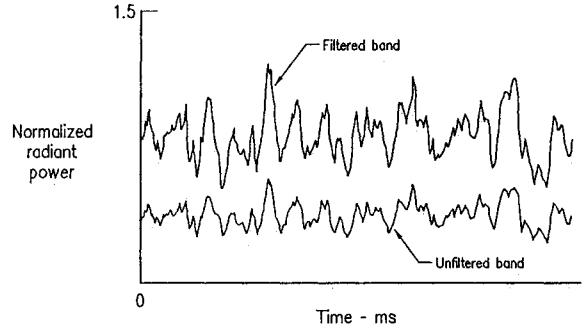

Fig. 2 Combustor radiance vs time for both measurement bands.

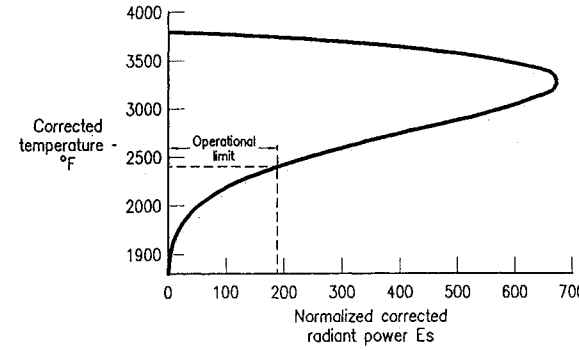

Fig. 3 Relationship between reflection-corrected blade temperature and reflection-corrected power.

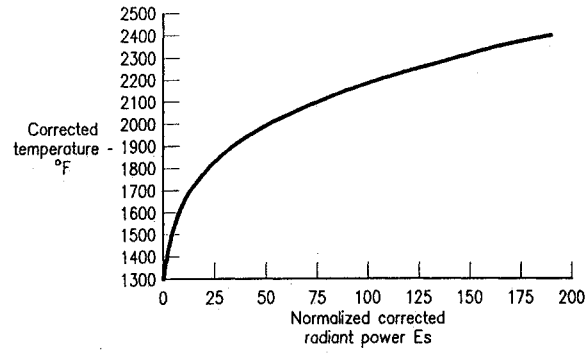

Fig. 4 Practical operating range for the DSAP algorithm.

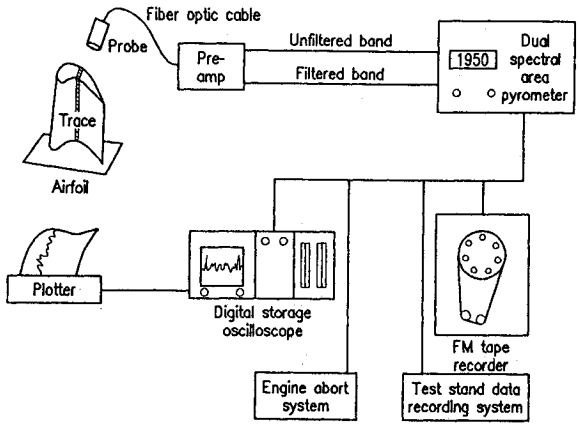

Fig. 5 Schematic of pyrometer system components.

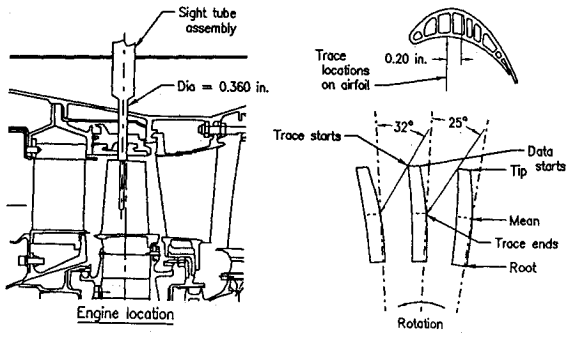

Fig. 6 Simple angle pyrometer installation.

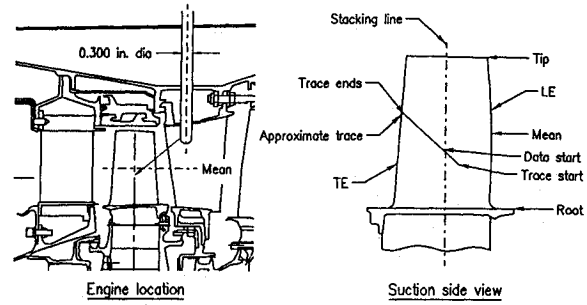

Fig. 7 Off-axis field of view pyrometer installation.

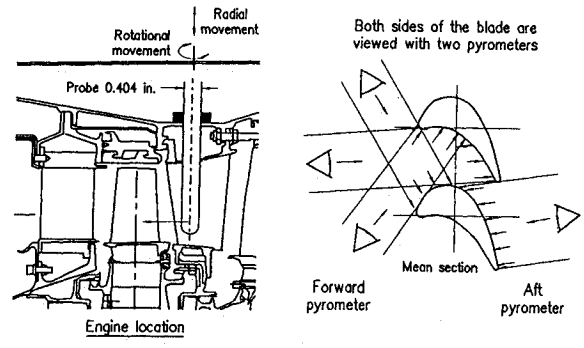

Fig. 8 Traversing and rotating mapping pyrometer installation.

nent overwhelms the blade emission. In any case, the results are the same; the indicated metal temperature is erroneously high. It is possible to correct this error by discarding the affected data and retaining the rest. Since the occurrence of the saturation is random with respect to turbine angular location, the discarded data for a given location may be replaced by valid data in subsequent revolutions.

The technique can be used for blade temperature profile determination as well as turbine overheating protection. Since data accuracy and frequency of temperature updates may vary considerably from one application to another, different signal processing algorithms are used. In both cases, however, the number of revolutions to be processed depends on the frequency of signal saturation. Saturation frequency can vary significantly between engine models. Consequently, the convergence of blade temperature values as a function of revolutions is determined first.

For turbine overtemperature protection, the average of the maximum individual temperatures for all the blades in the wheel is determined for use as part of the engine abort system. It is critical that processing time be kept to a minimum in order to update the result as quickly as possible. Computational time is minimized by sorting only the data in the vicinity of the maximum blade temperature. To speed processing further, all data are first corrected for reflection and then sorted. Results from typical development engines indicate that the average maximum blade temperature can be updated at least twice a second. Currently all data and signal processing are handled by a portable computer on the test stand. Although this procedure is acceptable for turbine average maximum temperature, it does not produce the best results for determining blade temperature profiles.

Blade temperature profiles are obtained by sorting the unfiltered band data, then correcting for reflection. Sorting the unfiltered band also sorts the reflection level present in the data, thus reducing the reflection correction error. Each retained unfiltered-band data point has an associated filtered-band data point acquired simultaneously. Both values are then used to correct for reflection. The process is performed for every blade of the turbine with data points acquired every 2 μs. Variations in turbine speed are corrected by normalizing all revolutions used in the data sorting process.

Pyrometer Engine Applications

Pyrometer Installations

The pyrometer system consists of three major components: radiation collecting optics, signal processor, and data acquisition system. Figure 5 depicts the arrangement of the system components.

Pyrometer installation techniques vary from engine to engine and are primarily a function of the type of data that is needed. Basically three types of installations are normally used: 1) simple or complex angle fixed, 2) periscope-type with variable sight angle, and 3) multiprobe traversing and rotating mapping. Examples of these installations are shown in Figs. 6, 7, and 8.

The simple or complex fixed angle installation requires a sight tube that penetrates the gas-path outer wall. In general, this includes the fan duct, the turbine case, and the blade outer air seal or vane platform. These installations are hard mounted. Trace shape and measurement location are a function of the type of installation, and corrections must be made for the relative growth of the cases and rotor shift. Rotor shift in most cases does not exceed 0.100 in. The periscope-type pyrometers in most applications are installed with a bayonet lock system that fits an inspection port plug. These units are well adapted to use in the field to inspect for deterioration or cooling-related anomalies. Temperature profiles for this type of pyrometer are generally difficult to define because of the probe view angle, rotor shift, radial runout, and installation tolerances.

The traversing rotating installations are the most complex and risky application since the probe penetrates the entire radial length of the flow path. The probe causes gas-path blockage that generates a vibratory excitation on the turbine

blades. This excitation increases the vibratory stresses of the turbine airfoils. In this case, data analysis is more complex because the engine actually experiences a measurable rematch (change in operating conditions) as a result of the flow-path blockage. However, this test provides the most useful data of all installations since up to 90% of surface area of a typical airfoil can be mapped. The percentage of mappable surface area is a function of engine size; generally the larger the engine, the higher the percentage of mapped surface area.

The probe housing assembly for all applications other than mapping is hard mounted to the engine case by either bolting or by using a quick disconnect bayonet lock system. This assembly contains the optical lens system and provisions for the purge gas used to avoid lens contamination and for probe cooling. The lens, generally a doublet, is custom designed to meet specific spot size and focal length requirements. Typically, spot sizes in diagnostic applications range from 0.060–0.125 in. in diameter. The housing, called the sight tube assembly, also accommodates the optic interface between the lens and the fiber optic transmission cable. The fiber optic cable transmits the radiation of the measurement spot from the probe to the detector-preamplifier assembly mounted on the engine shroud top. This module is water cooled to minimize electronic noise and drift. The primary function of the detector and preamplifier is to transform the radiative energy into a conditioned electrical signal to be transmitted over relatively long cable lengths without signal deterioration. The next part of the system is the DSAP signal processor located in the test stand control room. This unit contains the necessary electronic hardware to process the unfiltered and filtered signals and output the blade-corrected temperature in real time. Analog and digital versions of the processor are used. The digital version has a response time of 2.4 μs to 95% of a step input, whereas the analog version response occurs in 8 μs.

The data acquisition and support equipment necessary for the engine abort and diagnostic system are shown in Fig. 5. All

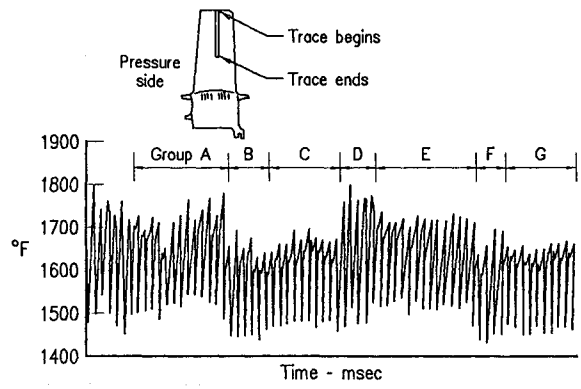

Fig. 9 Temperature trace for a rotor containing blades with different cooling designs.

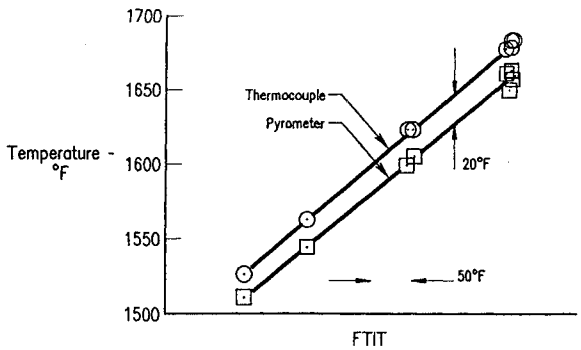

Fig. 10 Comparison between pyrometer and thermocouple indicated temperature.

pyrometer data are recorded continuously on a frequency modulation magnetic tape system. It is also fed directly to the main data recording center where the last minute of data are continuously saved in the event of an engine failure. For transient operation, the average maximum temperature is monitored on a strip chart.

The digital storage oscilloscope provides real-time traces of the entire rotor with sufficient resolution to distinguish individual blade profiles. For applications with high flame or radiation content, data sorting must be utilized. The technique is implemented using a portable computer system that processes the data to display temperature profiles or provide peak average temperature signals to a stand abort system in near real time. In the abort loop, peak metal temperatures are predetermined as governing either a durability or performance limit. This limit may not necessarily be a limit on a turbine component. If a predetermined limit is reached or exceeded, the engine or stand control may be programmed to reduce fuel flow to bring the measured metal temperature below the limit or it may initiate an idle trip. Under some circumstances, if the transient temperature change is very rapid, the control may trigger a complete shutdown, generally achieved by completely turning off the fuel valve. This abort or topping feature has more than once prevented engines from reaching overtemperature conditions.

A large number of internal geometries are tested simultaneously by configuring a turbine rotor with blades containing different cooling schemes and flow rates while maintaining the aerodynamics constant. Figure 9 shows the trace from such a turbine, normally referred to as rainbow rotor. Heat transfer designers are interested in the absolute level of local temperature for a given operating point; however, the intent of most rainbow rotors is to define the highest cooling effectiveness or most cost-effective cooling scheme. These rotors rapidly provide data to evaluate the effects of cooling level, hole-drilling technique, core geometry, and even surface roughness effects. Examination of the trace in Fig. 10 clearly shows not only a peak temperature range of almost 200°F but also shows distinct profile patterns. In this particular rotor, blades were grouped by configuration as indicated by the arrows above the traces.

Pyrometer Engine Data

The pyrometer system, whether used as a topper or as a cost-effective turbine-cooling development tool, has produced a great deal of needed data and has prevented several serious engine incidents. Good correlation between the pyrometer and thermocouple has been achieved for both cooled and uncooled airfoils. Table 1 summarizes the comparison between pyrometer and thermocouple measured temperature at two locations for cooled airfoils in the high pressure turbine. The reflection level fluctuated between 30–50% of the signal in the unfiltered channel. The imbedded thermocouple data were used to calculate the airfoil surface temperature at the location. The pyrometer data were corrected for reflection to the measured combustor radiance temperature and also corrected for burning particles in the field of view. For both cases the values shown in Table 1 are averages for a set of readings at steady-state conditions.

Figure 10 shows a comparison of thermocouple and pyrometer measured temperatures of an uncooled blade in the low-pressure turbine at various engine operating points. The discrepancy of these data is well within the accepted uncertainty band of both sensor systems and associated location tolerance.

Table 1 Comparison of pyrometer and thermocouple temperatures for surfaces with combustor reflection

Airfoil location	Pyrometer, °F	Thermocouple, °F
Midchord	1891	1898
Trailing edge	1838	1841

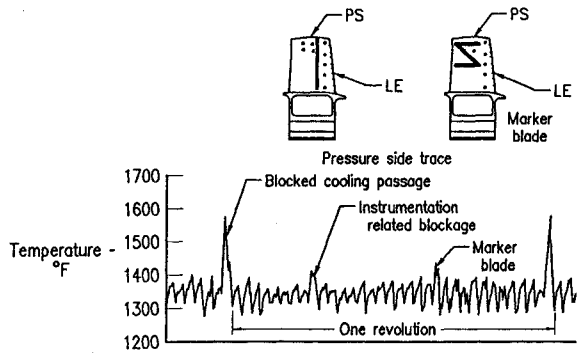

Fig. 11 Temperature trace of a high-pressure turbine with hot and marker blades.

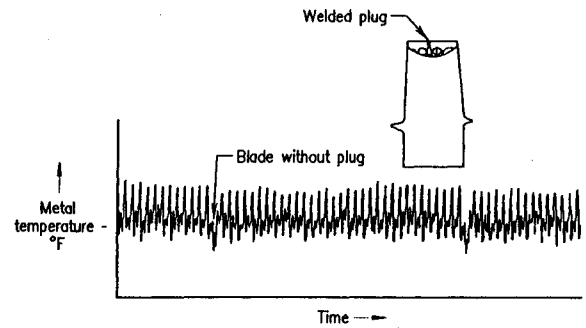

Fig. 12 Temperature trace of a high-pressure turbine with overcooled blade.

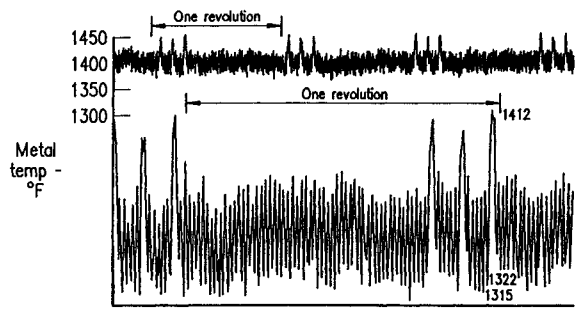

Fig. 13 Temperature trace obtained using pyrometer for field inspection.

Figure 11 shows a trace of a 5000-shaft horsepower engine high-pressure rotor viewing the pressure side of the blades. This trace identifies a hot blade caused by residual ceramic core material in the center of the multipass rear passage. This lack of cooling would have led to overheating at full power. The other hot blades experienced a partial passage blockage by an instrumentation wire in the supply passage, resulting in a cooling flow reduction. The blade in the figure identified as the marker blade contains a flame-sprayed aluminum oxide strip on the airfoil surface. This marker acts as a location and indexing feature. It quite accurately relates the trace to a radial location on the blade airfoil.

Figure 12 in this case identifies a colder than normal blade. This situation did not present a risk to the engine. On tear down, it was discovered that a core print weld had failed, thus increasing the coolant flow level by the presence of an oversized tip hole.

Figure 13 shows a trace of a second-stage turbine blade captured at part power during a test-stand checkout of a pyrometer system configured for field inspection. The pyrometer in this case is inserted in the aft turbine inspection port looking forward at the suction side of the second blade of

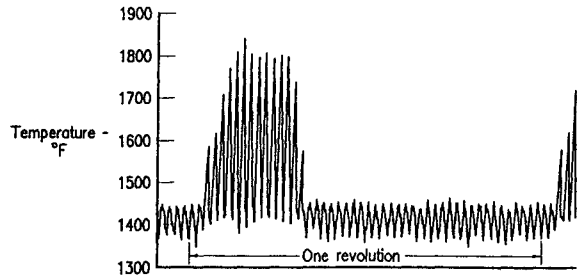

Fig. 14 Temperature trace resulting from blade tip rub.

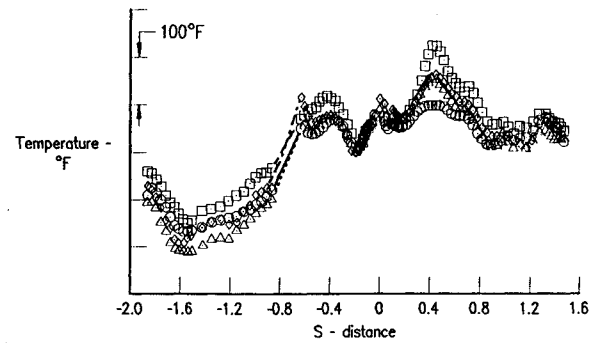

Fig. 15 Complete blade temperature profile obtained using mapping pyrometer.

the high turbine. The trace clearly indicates a cooling problem with three of the blades even at very low temperatures.

Figure 14 shows another trace taken at part power. The trace shows the heated blade tip immediately after a rub occurred between the blade tip and the stationary blade outer air seal.

Temperature isotherms for each blade are generated by compiling a series of individual temperature records. Figure 8 depicts the different views taken by a two-pyrometer installation typical in a full-mapping application. In addition to generating color isotherms of the blade airfoil, the mapping system generates temperatures profiles as shown in Fig. 15. The plot shows the temperature distribution along the blade chord at a constant span. The blade leading edge corresponds to zero; negative values to the blade suction side and positive values to the pressure side. In this case the plot shows the results for four different cooling configurations all tested simultaneously. Once the airfoil temperature data have been reduced, the turbine heat transfer designer can access and generate these types of plots for all blades in the rotor at any desired blade span within the range measurement.

Reflected radiation continues to limit pyrometry applications. Test experience has shown that the percentage of reflected radiation is dependent on engine-operating conditions. For example, core engines that are run in facilities with variable inlet temperature and pressure levels have shown that reflected radiation percentages increase with increasing pressure. Engines running at full intermediate sea-level takeoff have a higher percentage of reflected energy than would be observed at part power operation even though the radiance temperature remains relatively constant. The presence of flame in the pyrometer field of view is more frequent at higher power levels. Other factors that influence observed reflected energy are overall combustor length and combustor pattern factor where pattern factor is defined as average combustor temperature rise divided by maximum temperature rise. The percentage of reflected energy can range from 30–65% of the radiation in the unfiltered band for the same combustor configuration but different rig measured pattern factors. Older generation engines with longer combustor sections generally show lower reflected energy levels.

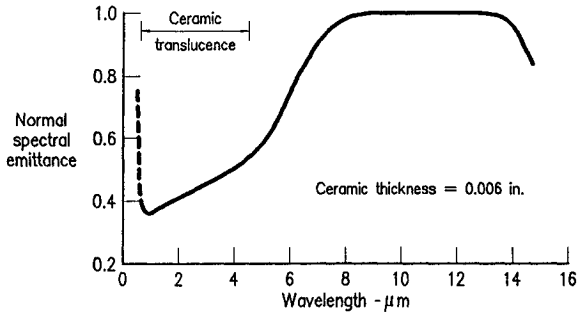

Fig. 16 Spectral emittance of a thermal barrier coating layer 0.006 in. thick over a metal substrate.

Pyrometry on Ceramics

Application of the DSAP technique to ceramic-coated components is limited by the radiative properties of these materials. The DSAP as currently configured operates in the 0.35–1.15 μ band as defined by silicon detectors. As noted earlier, the technique also assumes all surfaces to be gray and have high emissivity. Ceramic coatings do not meet these requirements. Coatings such as Yttria-stabilized Zirconia deposited on an underlayer of Ni-Cr-Al-Y, itself deposited on a metal substrate, generally have low spectrally dependent emittance in the wavelengths of interest. Figure 16 shows a typical plot of spectral emittance for this material. Emittance measurements reported in Ref. 3 indicate the ceramic coating to be translucent in the 1–5 μ region but opaque with a high emittance value (0.9) from 8–12 μ. The surface temperature could be measured by operating the pyrometer at these long wavelengths provided an adequate correction can be made for reflection. As stated earlier, the pyrometer operating bands are selected to have different sensitivity to reflected radiation. The bands are also selected to minimize the overall error, i.e., large corrections based on small signal differences must be avoided. Unfortunately, detectors sensitive to these wavelengths have inadequate response times or require a cryogenic environment. In order to map turbine blade temperatures, the system response should be no more than 8 μs to 95% of a step input. A detector such as Mercury-Cadmium-Telluride operating at $-385°$F (77 K) has the capability of operating at these wavelengths and response rates. Thermopiles and thermistors could be used for stationary components and other applications requiring slow response times. Currently the requirements of response time, signal to noise, and reliability in a jet engine environment are only readily met by silicon and Indium-Gallium-Arsenide detectors providing an operating band from 0.4 to 1.8 μ. At these wavelengths the surface material is translucent, with low wavelength-dependent emittance. If the resulting emittance of the ceramic coating as deposited on engine components is such that the combustor reflection does not overwhelm the emission from the blade, the present pyrometer could be used for engine health monitoring. Although the indicated temperature would be misleading, the relative magnitude of the temperature among similarly coated blades would serve to indicate hot or cold blades.

When correcting for high levels of reflection, with the gray surface assumption no longer being valid due to the dependence of the emittance on the thickness and application of the ceramic coating, it would be necessary to measure the spectral characteristics of the reflected radiation directly off the blade. The spectral measurement of the reflection component would be performed by using an additional spectral band. The three signals, in conjunction with an iterative algorithm, would calculate and update the spectral ratio of the reflected component. Sufficient processing time would be available since the rate of change of the reflected component ratio is several times slower than the blade-passing frequency. This measurement would reduce the overall measurement uncertainty to perhaps reasonable and useful bounds.

Conclusions

The pyrometer has been developed to be an accurate and cost-effective tool for obtaining the data required for turbine-cooling development. It has also provided substantial savings by preventing turbine failures in test engines and aircraft. The rate at which ceramic coatings are being introduced in the engine hot section presents a new pyrometry development challenge. Alternatives must be defined to overcome the material translucence, low emissivity, and corresponding high reflection. Work in progress involves measuring the emittance of these materials to evaluate various approaches consisting primarily of selecting new pyrometer spectral bands. Other approaches being considered are discussed in Ref. 2. These include active pyrometry and thermographic phosphors.

Acknowledgments

The pyrometer development effort was supported in part by the Air Force Contract F33657-84-C-2137 and by the Pratt and Whitney Division of United Technologies Corporation.

References

[1]Atkinson, W. H., and Strange, R. R., "Pyrometer Temperature Measurements in the Presence of Reflected Radiation," American Society of Mechanical Engineers, New York, ASME Paper 76-HT-74, Aug. 1976.

[2]Atkinson, W. H., and Strange, R. R., "Turbine Pyrometer for Advanced Engines," AIAA Paper 87-2011, July 1987.

[3]Liebert, C. H., "Emittance and Absorptance of NASA Ceramic Thermal Barrier Coating System," NASA TP 1190, June 1978.